Water Research 143 (2018) 599–607

Contents lists available at ScienceDirect

Water Research

journal homepage: www.elsevier.com/locate/watres

Co-oxidation of As(III) and Fe(II) by oxygen through complexation between As(III) and Fe(II)/Fe(III) species

Wei Ding [a], Jing Xu [a], Tao Chen [a], Chengshuai Liu [b, c, **], Jinjun Li [a], Feng Wu [a, *]

[a] Hubei Key Lab of Biomass Resource Chemistry and Environmental Biotechnology, School of Resources and Environmental Science, Wuhan University, Wuhan, 430079, PR China
[b] Guangdong Key Laboratory of Agro-environmental Pollution Control and Management, Guangdong Institute of Eco-environmental Science & Technology, Guangzhou, 510650, PR China
[c] State Key Laboratory of Environmental Geochemistry, Institute of Geochemistry, Chinese Academy of Sciences, Guiyang, 550081, PR China

ARTICLE INFO

Article history:
Received 5 March 2018
Received in revised form
15 June 2018
Accepted 30 June 2018
Available online 30 June 2018

Keywords:
Fe(II)/Fe(III)–As(III) complex
As(III) oxidation
Fenton-like reaction
Fe(IV) intermediate
Direct electron transfer

ABSTRACT

Previous studies have shown that the oxidation of Fe(II) by molecular oxygen can lead to the co-oxidation of As(III) at neutral pH. However, the mechanism of As(III) oxidation in the presence of Fe(II) with respect to the interaction between As(III) and Fe(II) is still unclear. In this work, we examined the oxidation of As(III) in the presence of Fe(II) in air-saturated water, which is affected by pH, co-existing phosphate, and scavengers (*tert*-butanol, superoxide dismutase, catalase and dimethylsulfoxide). Results confirm that the formation of the Fe(II)–As(III) complex (formation constant, $K_{Fe(II)-As(III)} = 10^{3.86}\,M^{-1}$) plays an extremely important role in the initial stage of As(III) oxidation at pH 7.25. The oxidation of Fe(II)–As(III) promotes the production of H_2O_2 and colloidal ferric hydroxide. H_2O_2 reacts with the Fe(II)–As(III) complex through oxidizing Fe(II) to Fe(IV), which then causes the partial oxidation (ca. 50%) of As(III). The other part of As(III) oxidation by H_2O_2 occurs, in the form of Fe(III)–As(III) complex, through direct electron transfer from As(III) to H_2O_2 but not through Fe(IV). This work provides new mechanistic insight into arsenic and iron redox chemistry in the environment and furthers our understanding of Fenton reactions at neutral pH.

1. Introduction

Fe(II) autoxidation by oxygen follows a stoichiometric relationship (eq (1)) and an apparent kinetic model (eq (2)) with an applicable pH range of 6–7.5 (Stumm and Lee, 1961), in accordance with the sequence of reactions in eqs (3)–(6) (Weiss, 1935). During Fe(II) autoxidation, reactive oxygen species (ROS), mainly $HO_2^{\bullet}/O_2^{\bullet-}$, H_2O_2, and $HO^{\bullet}$, are produced and depleted simultaneously. Some ligands or chelators with oxygen atoms favor complexing Fe(II) and stabilizing the product of Fe(III), thus decreasing the reduction potential of iron and promoting Fe(II) oxidation (Welch et al., 2002). Such complexes, symbolized as Fe(II)–L, can boost the production of ROS (eqs (7)–(10)) (Jones et al., 2015). The Fe(II) and ligands or chelators can be oxidized simultaneously by ROS (Lee et al., 2014). This complexation effect has been utilized to modify Fenton-like systems for the oxidation of contaminants.

$$Fe(II) + 1/4O_2 + 2OH^- + 1/2H_2O \rightarrow Fe(III)(OH)_3 \quad (1)$$

$$r_{Fe(II)} = k[Fe(II)]\left[OH^-\right]^2 p_{O_2} \quad k = 1.5(\pm 0.5) \times 10^{13}\ (M^{-2}\ min^{-1}\ atm^{-1}) \quad (2)$$

$$Fe(II) + O_2 \rightarrow Fe(III) + O_2^{\bullet-} \quad (3)$$

$$Fe(II) + O_2^{\bullet-} + 2H_2O \rightarrow Fe(III) + H_2O_2 + 2OH^- \quad (4)$$

$$Fe(II) + H_2O_2 \rightarrow Fe(III) + OH^- + HO^{\bullet}\ (\text{Fenton reaction}) \quad (5)$$

$$Fe(II) + HO^{\bullet} \rightarrow Fe(III) + OH^- \quad (6)$$

* Corresponding author. Guangdong Key Laboratory of Agro-environmental Pollution Control and Management, Guangdong Institute of Eco-environmental Science & Technology, Guangzhou, 510650, PR China.
** Corresponding author. Hubei Key Lab of Biomass Resource Chemistry and Environmental Biotechnology, School of Resources and Environmental Science, Wuhan University, Wuhan, 430079, PR China.
E-mail addresses: liuchengshuai@vip.gyig.ac.cn (C. Liu), fengwu@whu.edu.cn (F. Wu).

https://doi.org/10.1016/j.watres.2018.06.072
0043-1354/

$$Fe(II) + L \rightarrow Fe(II)\text{–}L \; K_{Fe(II)-L} = [Fe(II)\text{–}L]_{eq}/[Fe(II)]_{eq}[L]_{eq} \quad (7)$$

$$Fe(II)\text{–}L + O_2 \rightarrow Fe(III)\text{–}L + O_2^{\bullet -} \quad (8)$$

$$Fe(II)\text{–}L + O_2^{\bullet -} + 2H_2O \rightarrow Fe(III)\text{–}L + H_2O_2 + 2OH^- \quad (9)$$

$$Fe(II)\text{–}L + H_2O_2 \rightarrow Fe(III)\text{–}L + OH^- + HO^{\bullet} \quad (10)$$

where $r_{Fe(II)}$ is the oxidation rate of Fe(II), k is the rate constant, p_{O_2} is the partial pressure of oxygen, and $K_{Fe(II)-L}$ is the formation constant of Fe(II)–L complex.

Arsenic is a typical contaminant of groundwater and soils, mainly occurring in the inorganic forms arsenite (As(III)) and arsenate (As(V)), depending strongly on its redox chemistry (Oremland and Stolz, 2003; Sorg et al., 2014). The transformation of As(III) to As(V) is an important toxicity attenuation due to the higher toxicity of As(III). Iron is one of the major redox-sensitive metal elements affecting the transfer and/or transformation of arsenic species (Goldberg, 2002). Oxidation of As(III) in the presence of Fe(II) and dissolved oxygen (DO) is an important pathway for As(III) transformation, accounting for As(V) formation in air-exposed groundwater containing As(III) and Fe(II) (Hug and Leupin, 2003; Johnston and Singer, 2007). Co-oxidation of As(III) and Fe(II) is important not only to natural waters, but also to technical systems at neutral pH (Hug and Leupin, 2003). According to eqs (3)–(6), H_2O_2 coupled to Fe(II), known as a Fenton reaction, leads to As(III) oxidation and formation of co-precipitate products, ferric hydroxide and ferric arsenate (Fe(III)–As(V)). This mechanism has been widely used to remove arsenic from arsenic-rich groundwater or sewage. Simple, and inexpensive methods or technologies, especially for drinking water treatment in rural areas, include Fe(II)/O_2 or Fe(II)/H_2O_2 (Hug et al., 2001; Hug and Leupin, 2003), Fe(0)/O_2 or Fe(0)/H_2O_2 (Katsoyiannis et al., 2008, 2015; Pang et al., 2011), and Fe(II) (hydr)oxide/O_2 or Fe(II) (hydr)oxide/H_2O_2 (Ona-Nguema et al., 2010; Shao et al., 2016).

Hug and co-workers (Hug et al., 2001; Hug and Leupin, 2003; Katsoyiannis et al., 2008) suggested that although Fe(II) autoxidation possibly produces ROS, ferryl iron (Fe(IV)) dominates $HO^{\bullet}$ as the main oxidant for As(III) as the pH increases from 3.5 to 7.5 in aerated solutions (6.6 μM As(III), 0.1–20 μM Fe(II), pH 7.0 or 7.5). In neutral Fenton reactions (pH 6.0–7.0), Fe(IV) has been identified as the Fenton intermediate by using $(CH_3)_2SO$ (Bataineh et al., 2012). Pang et al. (2011) ruled out Fe(IV) as an active Fenton intermediate, and thought that $HO^{\bullet}$ and heterogeneous surface reactions were responsible for As(III) oxidation in the Fe(0)/O_2 system over a wide pH range. However, the possible effect of As(III) on Fe(IV) formation (e.g., complexation) and whether only Fe(IV) is responsible for As(III) oxidation during Fe(II) autoxidation in neutral aerated solutions have not been clarified.

In decades, the complexation between As(III) and iron (hydr) oxides (Banerjee et al., 2008; Manning et al., 1998), as well as As(III) oxidation on colloidal ferric hydroxide (CFH) via photoinduced ligand-to-metal-charge transfer (Xu et al., 2014), has been proposed. However, few studies have reported the complexation between As(III) and Fe(II) possibly because of 1) the normally poor complexing property of Fe(II) and 2) the low stability and sensitivity to DO of the Fe(II)–As(III) complex. Two groups demonstrated Fe(II)–As(III) complex formation at neutral pH based on extended X-ray absorption fine structure (EXAFS). Thoral et al. (2005) found As(III) inner-sphere complexes on ferrous hydroxide particles formed at pH 7, which were present at extremely high concentrations of both As(III) (0.2 M) and Fe(II) (0.2 M). Ona-Nguema et al. (2009) prepared a model compound, amorphous Fe(II)–As(III) hydroxide (co-precipitate), with 0.3–0.9 mM As(III) and 3 mM Fe(II) at pH 7, as well as provided EXAFS evidence for the multinuclear As(III) complexes at the edges of layered $Fe(OH)_2$ nanoparticles. Though they proposed the complexation between Fe(II) and As(III) at high concentrations, the possibility of Fe(II)–As(III) complex formation at lower concentrations of As(III) and Fe(II) and the mechanism of co-oxidation of As(III) and Fe(II) through this complex remain unclear.

This work is designed to provide mechanistic insight into the co-oxidation of Fe(II) and As(III) by DO in aqueous solutions at near-neutral pH. The specific aims are (i) to test the hypotheses that As(III) oxidation in the presence of Fe(II) and oxygen occurs through the formation of an Fe(II)–As(III) complex; (ii) to clarify the pathways of co-oxidation of As(III) and Fe(II); and (iii) to evaluate the relative contributions of ROS, Fe(IV), and direct electron transfer from As(III) to H_2O_2. This work may aid in understanding the co-oxidation of Fe(II) and As(III) in groundwater exposed to air and the mechanism for a circumneutral Fenton-like system.

2. Materials and methods

2.1. Chemicals and materials

All chemicals were of analytical reagent grade and were used without further purification unless noted otherwise. $NaAsO_2$ (99.5%) was obtained from Gracia Chemical Technology Co. Ltd. (Chengdu, China) and used after 24 h of drying in desiccators. $Na_2HAsO_4 \cdot 7H_2O$ was purchased from Alfa Aesar (Ward Hill, MA, USA). $FeSO_4 \cdot 7H_2O$, $Fe_2(SO_4)_3$, NaOH, H_2SO_4, HCl, KBH_4, KOH, NaH_2PO_4, Na_2HPO_4, NH_4F, CH_3COOH, CH_3COONa, ascorbic acid, 2,2′-dipyridyl (DP), dimethylsulfoxide (DMSO), tiron, H_2O_2 (30% w/w) and phenanthroline were purchased from Sinopharm Chemical Reagent Co. Ltd. (Shanghai, China). Piperazine-*N*,*N*′-bis(2-ethanesulfonic acid) (PIPES), 5,5-dimethyl-1-pyrroline-*N*-oxide (DMPO), superoxide dismutase (SOD), catalase (CAT), *N*,*N*-diethyl-*p*-phenylenediamine (DPD), and peroxidase (POD) were purchased from Internet Aladdin Reagent Database Inc. (Shanghai, China). *tert*-Butanol (TBA) was purchased from Shanghai Shiyi Chemicals Reagent Co. Ltd. Solutions except those of Fe(II) were prepared using fresh ultrapure water 18 MΩ cm from a water purification system (Liyuan Electric Instrument Co., Beijing, China) and stored at 4 °C. Stock solutions of Fe(II) were prepared at 25 °C immediately prior to use and adjusted to pH 4 by using H_2SO_4 to prevent Fe(II) autoxidation.

2.2. Co-oxidation of As(III) and Fe(II) by O_2

A reaction solution containing PIPES, $NaNO_3$, Fe(II), and As(III) was stirred with N_2 bubbling for at least 30 min in a water-jacketed reactor at 25 °C. Co-oxidation of As(III) and Fe(II) was launched by sparging compressed air (1 L min^{-1}, 20.8% v/v O_2 and 79.2% v/v N_2). Then the samples were taken for analysis at certain time intervals. All the operations were conducted in dark. $NaNO_3$ was used to fix the ionic strength. As one kind of noncoordinating tertiary amine buffers, the PIPES buffer was selected for pH control (optimum pH of 6.1–7.5), because it does not form complexes with Fe(II)/Fe(III) and can be used to control neutral pH in air-saturated water containing Fe(II)/Fe(III) and As(III) (Keenan and Sedlak, 2008; Pang et al., 2011). The addition of PIPES had no significant interference on the mechanism of Fe(II) autoxidation in this work (Fig. S1 and S2 in the Supplementary Information (SI)). The concentration of PIPES buffer was about 100 times greater than that of the limiting reagents so as to hold the pH at the desired value without altering the chemistry. The pH decrease of the reaction solution was less than 0.3 units for all experiments.

2.3. Complexing competition and radical scavenging assays

Experiments were conducted to confirm the effect of complexing competitors and radical scavengers on the co-oxidation of Fe(II) and As(III). The operation and reaction conditions were identical to those in section 2.2 besides the addition of complexing competitors or radical scavengers in N_2 bubbling period. The complexing competitors included phosphate, DP and tiron. The radical scavengers included TBA, CAT, SOD and DMSO.

2.4. Co-oxidation of As(III) and Fe(II)/Fe(III) by H_2O_2

A reaction solution containing PIPES, $NaNO_3$, Fe(II)/Fe(III), and As(III) was stirred with N_2 bubbling for at least 30 min before and during reaction in a water-jacketed reactor at 25 °C. Co-oxidation of As(III) and Fe(II)/Fe(III) was launched by adding specific amount of H_2O_2. The other operation was identical to that in section 2.2.

2.5. Analytical methods

The arsenic speciation (As(III) and As(V)) was simultaneously analyzed by liquid chromatography–hydride generation–atomic fluorescence spectrometry (LC–HG–AFS; Bohui Innovation Technology Co., Ltd., Beijing, China). The Fe(II) concentration was measured similar to our previous work (Wang et al., 2013). Briefly, the Fe(II) concentration was analyzed by adding the chelating agent 1,10-phenanthroline and then measuring the absorbance of the Fe(II)–$(1,10\text{-phenanthroline})_3^{2+}$ complex by spectrophotometry at 510 nm (Shimadzu UV-1601, Japan). To terminate the co-oxidation of As(III) and Fe(II) and detect the total concentrations of As and Fe (i.e., the summation of the dissolved, adsorbed and precipitated forms), samples were taken for analysis at certain time intervals and added quickly to colorimetric tubes containing 1 mL HCl solution (1:1 v/v) diluted with fresh ultrapure water to 10 mL. The concentrations of dissolved As and Fe were determined by centrifugation to separate the colloids in the samples without acidification. The concentrations of adsorbed As and Fe were obtained after subtracting dissolved As and Fe concentrations from total As and Fe concentrations. [As(III)] and [Fe(II)] referred to total concentrations of As(III) and Fe(II), i.e. the summation of the dissolved, adsorbed and precipitated forms unless noted otherwise.

The Fe(II)/Fe(III) species distribution versus pH was simulated by Medusa software. The redox potentials of Fe(III)/Fe(II) and As(V)/As(III) were determined by cyclic voltammogram experiments with an electrochemical workstation (CHI600E, CH Instruments Ins.). Free radicals produced during Fe(II) autoxidation were detected by Electron spin resonance (ESR) spectroscopy using a Japan Electron Optics Laboratory Co. Ltd. FA200 spectrometer. The concentration of H_2O_2 was determined using DPD photometric method at a wavelength of 551 nm (Wang et al., 2013). The formation constant of Fe(II)–As(III) complex at neutral pH was calculated using pH metric titrations method proposed by Bjerrum (1941) and modified by Irving and Rossotti (1954). Except for special description, the initial reaction rate (expressed as r) was determined from the linear fit of the plot of concentration versus reaction time within 0–5 min.

The details of analytical methods have been described in SI.

3. Results and discussion

3.1. pH effect on co-oxidation of As(III) and Fe(II)

The effect of pH on the co-oxidation of As(III) (Fig. S3a) and Fe(II) (Fig. S3b) was investigated at pH 6.0–8.0. For both As(III) and Fe(II) oxidation, the apparent pH dependence of initial oxidation rates of As(III) ($r_{As(III)}$) and Fe(II) ($r_{Fe(II)}$) followed the kinetic model (eq. (2)) shown in Fig. S3c, which implies that $r_{As(III)}$ and $r_{Fe(II)}$ have a potential relationship. As expected, correlation analysis confirmed a linear positive correlation between $r_{As(III)}$ and $r_{Fe(II)}$ (Fig. 1) as the pH increased from 6 to 8, with a slope, $r_{Fe(II)}/r_{As(III)}$, of ca. 20. The slope is twice the initial concentration ratio of [Fe(II)]/[As(III)], indicating that the oxidation efficiency of As(III) is stoichiometrically lower than that of Fe(II). As shown in Fig. S3c, As(III) accelerated Fe(II) oxidation rates. Thus, we determined the correlation between the increment of the Fe(II) oxidation rate ($\Delta r_{Fe(II)}$, described in eq (11)) and $r_{As(III)}$. Fig. 1 shows a linear positive correlation between $\Delta r_{Fe(II)}$ and $r_{As(III)}$, with a slope of ca. 4.

$$\Delta r_{Fe(II)} = r_{Fe(II)} - r_{Fe(II)0} \quad (11)$$

where $r_{Fe(II)}$ and $r_{Fe(II)0}$ are the initial oxidation rates of Fe(II) with or without As(III) respectively. $\Delta r_{Fe(II)}$ is the increment of the Fe(II) oxidation rate after addition of As(III).

We simulated the species distribution of Fe(II) (Fig. S4) using Medusa software, ignoring the potential effect of As(III). Millo (1985) proposed that the formation of $Fe(OH)_2$ species at pH above 6 is a key step in Fe(II) oxidation. This is reasonable with respect to the concentration limit of Fe(III) free ion (ca. 10^{-14} M) at pH 6 (10^{-8} M [OH^-]), which depends on the solubility product constant ($pK_{sp} = 38.55$) of $Fe(OH)_3$ (precursor of CFH) (Speight, 2005). The same pH threshold (6.0) was also observed in As(III) oxidation to As(V) (Fig. S3c). Therefore, As(III) oxidation in nature depends on Fe(II) oxidation although the former apparently enhances the latter. To achieve significant oxidation of As(III) in a more stable Fe(II)/Fe(III) solution, we fixed the pH at 7.25 for all succeeding experiments.

3.2. Role of complexation between As(III) and Fe(II)/Fe(III)

Phosphate was added to the reaction solution to investigate its effect on the co-oxidation of As(III) and Fe(II). Fig. 2a shows that phosphate slightly enhanced Fe(II) oxidation because of the formation of relatively labile dissolved ferrous phosphate complexes at pH 6.75 (Johnston and Singer, 2007). Whereas, Fig. 2b shows that phosphate prevented almost all As(III) oxidation as the phosphate concentration increased to 250 μM. In Fe(II) solution containing 250 μM phosphate (5-fold higher than Fe(II)), only about 32% of Fe(II) formed iron(II)–phosphate complexes ($FeHPO_4$, $FeH_2PO_4^+$, or $Fe_3(PO_4)_2$) in the absence of As(III) at pH 7.25 calculated by Medusa

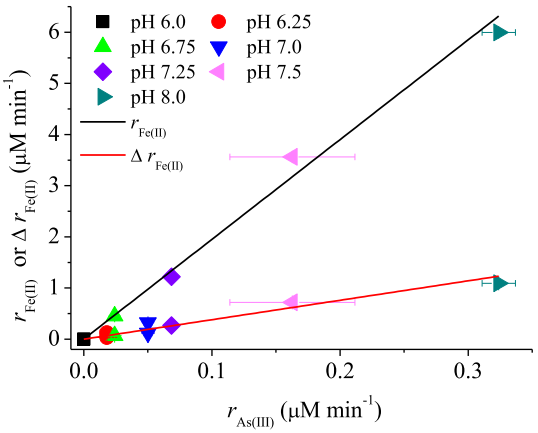

Fig. 1. Changes in the initial oxidation rates of As(III) ($r_{As(III)}$) and Fe(II) ($r_{Fe(II)}$) versus pH (6–7.5), and the relationship between $r_{As(III)}$ and $r_{Fe(II)}$ or $\Delta r_{Fe(II)}$. Conditions: [As(III)] = 5 μM, [Fe(II)] = 50 μM, [PIPES] = 5 mM, [$NaNO_3$] = 10 mM, p_{O_2} = 0.208 atm. $\Delta r_{Fe(II)}$ is the increment of Fe(II) oxidation rate with and without As(III).

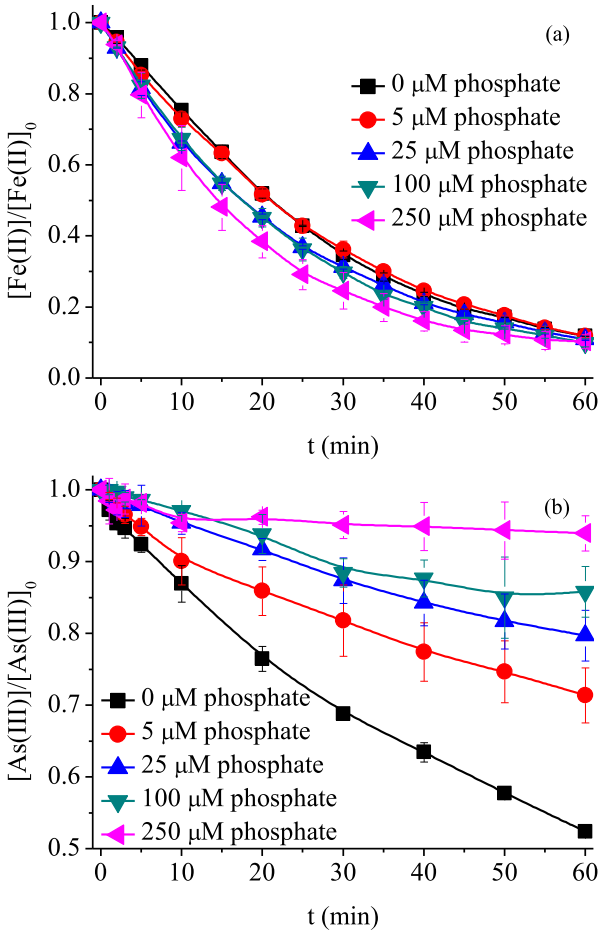

Fig. 2. Changes in Fe(II) (a) and As(III) (b) concentrations in the presence of phosphate. Conditions: [As(III)] = 5 μM, [Fe(II)] = 50 μM, [PIPES] = 5 mM, [$NaNO_3$] = 10 mM, [Phosphate] = 0–250 μM, pH 7.25.

software (Fig. S5a). About $10^{-12.1}$ M $Fe(OH)_2$ remained, which is close to the amount obtained without phosphate (Fig. S4). Formation of $FePO_4$•$2H_2O$ rather than CFH (Fig. S5b) also limited As(III)–CFH complexation. Since phosphate has a strong ability to complex with Fe(II)/Fe(III) and a chemical behavior similar to that of As(III) and As(V) (Raven et al., 1998; Xu et al., 2014), phosphate could compete with As(III) in complexation with Fe(II)/Fe(III). Therefore, the inhibitory effect was not only due to the formation of iron(II)/(III)–phosphate or scavenging of $HO^•$ radical by phosphate (rate constant < 10^7 M^{-1} s^{-1}), but also probably due to the competition of complexation between phosphate and As(III) with Fe(II) or Fe(III) (eqs (12) and (13)). As(III) reacts with $HO^•$ radical at a much higher reaction constant (8.5×10^9 M^{-1} s^{-1}) (Xu et al., 2014), thus we considered that As(III) might complex with Fe(II) or Fe(III) when $Fe(OH)_2$ species or CFH formed and that oxidation of As(III) occurred after these complexes formed.

$$\text{Fe(II)} + \text{As(III)} \rightleftharpoons \text{Fe(II)–As(III) complex} \quad (12)$$

$$\text{Fe(III)} + \text{As(III)} \rightleftharpoons \text{Fe(III)–As(III) complex} \quad (13)$$

The chelator DP favors the binding of Fe(II) ions over that of Fe(III) ions. This step forms $Fe(DP)_3^{2+}$ in solution, which exhibits no ability for activating oxygen (Li et al., 2004). Thus, DP was added to confirm the effect of Fe(II) autoxidation on As(III) oxidation. As shown in Fig. S6a and b, As(III) oxidation and Fe(II) oxidation were simultaneously and almost completely inhibited as the concentration of DP increased up to 5-fold that of Fe(II). This result is consistent with the work of Katsoyiannis et al. (2008), showing that DP interrupts reactions of Fe(II) with O_2 and H_2O_2. This result is also consistent with the very low concentrations of reactive $Fe(OH)_2$ species in 50 μM Fe(II) solution containing 250 μM DP at pH 7.25 (Fig. S5c). Therefore, the complex between Fe(II) and As(III) remained the ability for activating oxygen.

Because complexation may change the Fe(III)/Fe(II) or As(V)/As(III) reduction potentials, we conducted cyclic voltammetry measurements in the absence of oxygen. After As(III) complexation with Fe(II), the Fe(III)/Fe(II) reduction potential decreased from 0.072 to −0.11 V vs. a saturated calomel electrode (SCE) in Fig. S7a. This result agrees with the decrease in Fe(III)/Fe(II) reduction potential due to chelators complexation with Fe(II) via oxygen atoms (Welch et al., 2002). Meanwhile, this complexation increased the As(V)/As(III) reduction potential from 0.68 to 0.97 V vs. SCE (Fig. S7b), suggesting that As(III) oxidation with Fe(II) is more difficult than that without Fe(II). This finding seemingly contradicts the fast As(III) oxidation in the presence of Fe(II). Thus, some oxidants should be generated to overcome the higher As(V)/As(III) reduction potential.

3.3. Role of ROS in the co-oxidation of As(III) and Fe(II)

According to the results and discussions above, the oxidation of As(III) might occur by ROS ($HO^•$, H_2O_2, $O_2^{•-}$, or other oxidizing intermediates) that were formed as intermediates during the Fe(II) oxidation by O_2. Thus, the presence of a scavenger could inhibit the co-oxidation of As(III) and Fe(II) by quenching ROS. Therefore, verification experiments were conducted by adding ROS scavengers to inhibit the possible action of radicals. TBA was used as a probe compound for $HO^•$ in the photooxidation of As(III) through the surface complexation with nascent colloidal ferric hydroxide, and its concentration (20000-fold that of As(III)) was enough to quench almost all $HO^•$ due to the reaction constant ($k_{HO•/TBA}$ = $(3.8–7.6) \times 10^8$ M^{-1} s^{-1}) (Xu et al., 2014). Fig. S8 shows almost no inhibition of oxidation of As(III) or Fe(II) in the presence of excess TBA, which is in agreement with the results of experiments using 2-propanol as $HO^•$ scavenger (Hug and Leupin, 2003). In addition, ESR spectroscopy showed no signals of DMPO–OH adduct during the co-oxidation of As(III) and Fe(II) in the presence of DMPO (Fig. S9). These results thus confirm that $HO^•$ is not the key oxidant for As(III) or Fe(II).

CAT could decompose H_2O_2 at neutral pH with a reaction constant of 7.9×10^6 M^{-1} s^{-1} and was used to identify the generation of H_2O_2 during Fe(II)–polyphosphate complex oxidation by O_2 (Biaglow and Kachur, 1997). Thus, CAT was added to the reaction solution to investigate the inhibitory effect. Significant inhibition of co-oxidation of both As(III) (Fig. 3a) and Fe(II) (Fig. 3b) was observed with 100–500 U mL^{-1} CAT solution. As the concentration of CAT was increased to 500 U mL^{-1}, Fe(II) oxidation was not completely inhibited ($r_{Fe(II)}$ decreased from 1.22 to 0.25 μM min^{-1}), whereas As(III) oxidation was almost all inhibited ($r_{As(III)}$ decreased from 0.069 to 0.0095 μM min^{-1}). These results demonstrate that H_2O_2 is crucial to the co-oxidation of As(III) and Fe(II) in neutral solution. H_2O_2 was the only important oxidant for As(III) oxidation, while molecular oxygen was also another important oxidant for Fe(II) oxidation. The yields of H_2O_2 in Fe(II) solutions with or without As(III) were analyzed along with the autoxidation reactions. Fig. 3c shows that the initial reaction rate (within 0–10 min) and final concentration (at 60 min) of H_2O_2 in the presence of As(III) (0.31 μM min^{-1} and 5.4 μM) are markedly higher than those in the absence of As(III) (0.14 μM min^{-1} and 1.7 μM). This result implies that As(III) acts as a ligand for Fe(II), thus enhancing the production of H_2O_2.

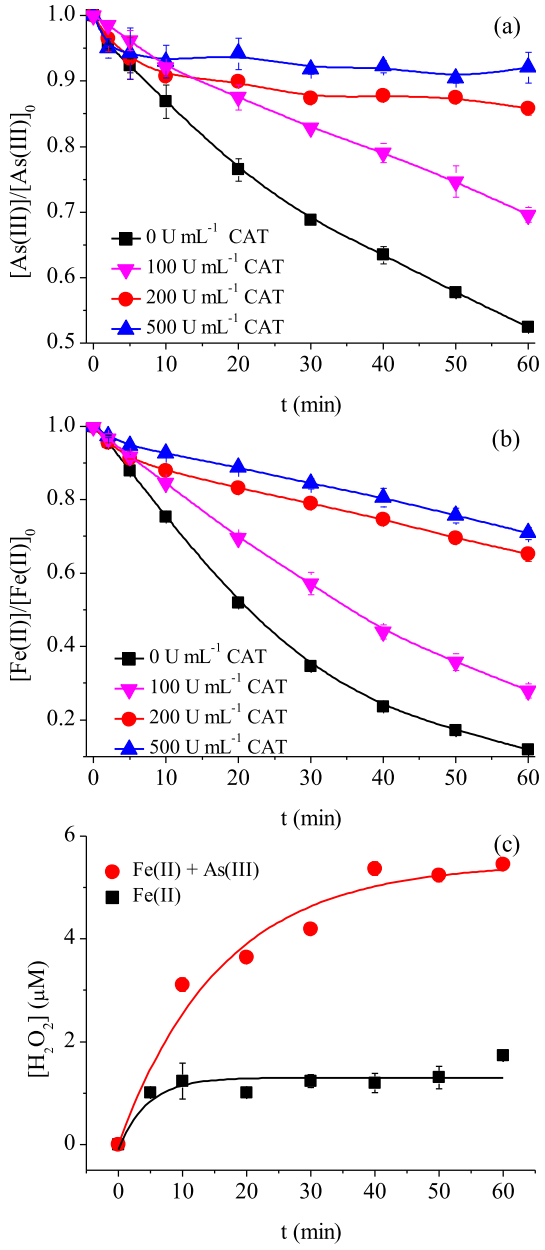

Fig. 3. Changes in As(III) (a) and Fe(II) (b) concentrations in the presence of CAT; (c) Yield of H_2O_2 during the oxidation of Fe(II) with or without As(III). Conditions: [As(III)] = 5 μM, [Fe(II)] = 50 μM, [PIPES] = 5 mM, [$NaNO_3$] = 10 mM, [CAT] = 0–500 U mL^{-1}, pH 7.25.

Another ROS, $HO_2^{\bullet}$ or $O_2^{\bullet-}$, is possibly produced during autoxidation of Fe(II); the neutral pH causes only $O_2^{\bullet-}$ to be the predominant species, as dictated by the acid dissociation constant ($pK_a = 4.8$) of $HO_2^{\bullet}/O_2^{\bullet-}$ reaction (Wood, 1988). SOD can react with $HO_2^{\bullet}/O_2^{\bullet-}$ with a high reaction constant of $6.1–24 \times 10^8\ M^{-1}\ s^{-1}$ and was used to testify the generation of $O_2^{\bullet-}$ during Fe(II)–polyphosphate complex oxidation by O_2 (Biaglow and Kachur, 1997). Thus, SOD was added to the reaction solution to investigate the effect of $O_2^{\bullet-}$ on the co-oxidation of As(III) and Fe(II). Fig. S10 shows that the oxidation of neither As(III) nor Fe(II) can be changed even by increasing the SOD concentration up to 96 U mL^{-1}. This suggests that free $O_2^{\bullet-}$ plays a minor role in the production of H_2O_2 or oxidation of As(III) and that generation of H_2O_2 can be based on the two-electron reduction of molecular oxygen via formation of an ions complex ($Fe^{3+}\bullet\ O_2^{2-}\bullet\ Fe^{3+}$), which is stabilized by Coulombic forces and may break up to form H_2O_2 (Weiss, 1953).

3.4. Oxidation of As(III) via reaction between Fe(II)–As(III) complexes and H_2O_2

Direct oxidation of As(III) by H_2O_2 in the absence of Fe(II) is hardly possible because of the very low reaction rate constant ($k = 5.5 \times 10^{-3}\ M^{-1}\ s^{-1}$) (Wang et al., 2013), unless the H_2O_2 concentration is high enough (e.g., several millimolar). Without iron, no oxidation of As(III) was observed (Fig. S11) at the maximal concentration of H_2O_2 (5.4 μM) found in the As(III) solution containing Fe(II) in this work. However, when we added H_2O_2 at various concentrations to the deoxygenated solutions containing Fe(II) and As(III), co-oxidation of As(III) and Fe(II) occurred, as shown in Fig. 4a. In this case, co-oxidation of As(III) and Fe(II) occurred very quickly and terminated within 5 min, reaching slopes

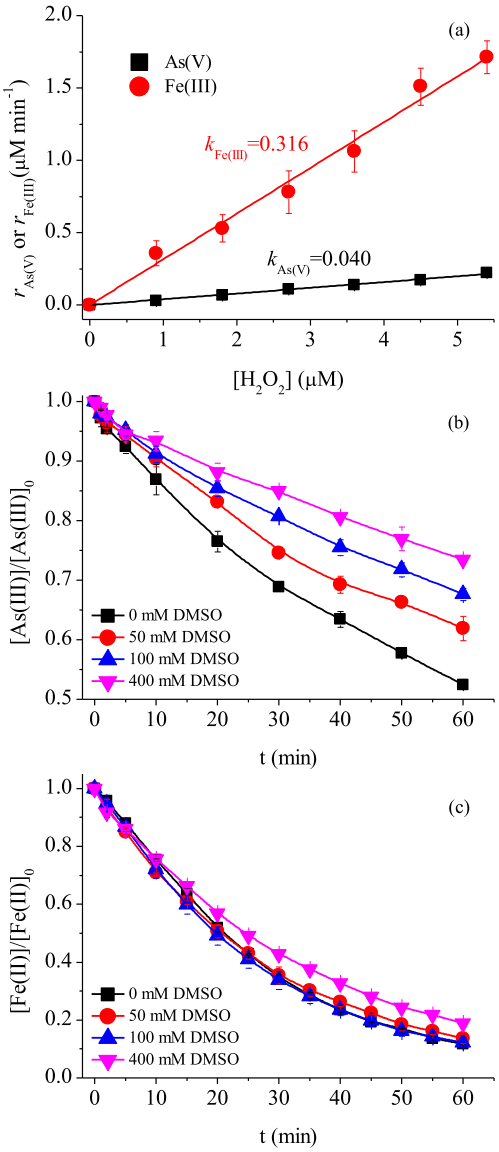

Fig. 4. (a) Changes in initial generation rates of As(V) ($r_{As(V)}$) and Fe(III) ($r_{Fe(III)}$) at different concentrations of H_2O_2 under a nitrogen atmosphere. Changes in As(III) (b) and Fe(II) (c) concentrations during the co-oxidation in the presence of DMSO. Conditions: [As(III)] = 5 μM, [Fe(II)] = 50 μM, [PIPES] = 5 mM, [$NaNO_3$] = 10 mM, [DMSO] = 0–400 mM, pH 7.25.

of 0.040 ($k_{As(V)} = r_{As(III)}/[H_2O_2]$) and 0.316 ($k_{Fe(III)} = r_{Fe(II)}/[H_2O_2]$), respectively. Moreover, the stoichiometries of oxidized As(III) and Fe(II) relative to H_2O_2 are 0.20 ($k_{As(V)} \times t = 0.040 \times 5$) and 1.58 ($k_{Fe(III)} \times t = 0.316 \times 5$), respectively. The initial rate of H_2O_2 reaction was 0.31 μM min^{-1} (Fig. 3c), thus the calculated $r_{As(III)}$ was 0.062 μM min^{-1} (0.20 × 0.31 μM min^{-1}), which is very close to that obtained using Fe(II) solution containing oxygen at pH 7.25 (0.069 μM min^{-1} in Fig. S3c). As the production rates of H_2O_2 increased from 0.14 to 0.31 μM min^{-1} after the addition of As(III) (Fig. 3c), the increased Fe(II) oxidation rate was calculated to be 0.27 μM min^{-1} (1.58 × 0.17 μM min^{-1}), which is also identical to the calculated $\Delta r_{Fe(II)}$, as shown in Fig. 1. Thus, one important conclusion that can be drawn, is that As(III) oxidation and the enhancement of Fe(II) oxidation during co-oxidation of As(III) and Fe(II) are exclusively attributed to the increased production of H_2O_2.

Along with the production of H_2O_2, As(III) oxidation in Fe(II) solutions at neutral pH comprises the neutral Fenton oxidation of As(III). Since HO• does not cause As(III) oxidation as reconfirmed in this work, the proposed reaction involving Fe(IV) (Hug and Leupin, 2003) should be demonstrated. DMSO reacts with Fe(IV) by oxygen atom transfer and yields dimethyl sulfone, whereas it reacts with hydroxyl radicals and generates methyl sulfinic acid and ethane. Thus, DMSO was used to verify the existence of Fe(IV) in Fenton reaction (Bataineh et al., 2012) and heterogeneous Fe(0)/O_2 systems containing As(III) (Pang et al., 2011). Hence, DMSO could be used as a scavenger for Fe(IV) in the absence of HO• in this work. Excess DMSO (400 mM) inhibited most of As(III) oxidation for 50 μM Fe(II) and 5 μM As(III) in the presence of 5.4 μM H_2O_2 under a nitrogen atmosphere (Fig. S12), which indicates that the Fe(IV) is the dominant oxidant for As(III) in neutral Fenton reaction. Fig. 4b shows that excess DMSO (400 mM) decreased the As(III) initial oxidation rate by approximately 50% (from 1.22 to 0.064 μM min^{-1}), which indicates that half of the As(III) oxidation is through reaction with Fe(IV). There must be other pathways of As(III) oxidation not via Fe(IV). Whereas excess DMSO did not significantly inhibit Fe(II) oxidation (Fig. 4c), which implies that Fe(II) oxidation did not occur via the Fe(IV) pathway. We thus propose that half of As(III) oxidation by H_2O_2 occurred via the Fe(IV) pathway (eqs (14) and (15)) and that the increased Fe(II) oxidation by H_2O_2 occurred through Fe(II)–As(III)/As(V) complexes (eqs (16) and (17)). To testify this proposal that the increased Fe(II) oxidation by H_2O_2 occurs through Fe(II)–As(III) complexes, Fe(II) oxidation by H_2O_2 with or without As(V) under a nitrogen atmosphere were recorded in Figs. S13 and S14, respectively. As expected, Fig. S13 demonstrates the negligible oxidation of 50 μM Fe(II) by 5.4 μM H_2O_2 in the absence of As(III)/As(V) and oxygen. An increase in H_2O_2 concentration (e.g., 1- to 10-fold that of the Fe(II) concentration, 54–540 μM) can lead to Fe(II) oxidation (ca. 10–60%). Therefore, reactions in eqs (18)–(20) hardly occurred at the low concentration of H_2O_2 produced during co-oxidation of As(III) and Fe(II) in this work. Meanwhile, Fig. S14 demonstrates that the reaction in eq (17) was very slow ($r_{Fe(II)} = 0.07$ μM min^{-1}) even for 50 μM Fe(II) and 5 μM As(V) in the presence of 5.4 μM H_2O_2 under a nitrogen atmosphere. Thus, the reaction in eq (16) is responsible for most increased Fe(II) oxidation. Evidently, DMSO can inhibit As(III) oxidation in eqs (14) and (15) by scavenging Fe(IV), but is unable to inhibit Fe(II) oxidation in eq (16) or (17). These reactions mainly take place on the surface of CFH once the reactions start. The final products are CFH and insoluble colloidal $FeAsO_4$ in solution.

$$\text{Fe(II)–As(III) complex} + H_2O_2 \rightarrow \text{Fe(IV)–As(III) complex} \quad (14)$$

$$\text{Fe(IV)–As(III) complex} \rightarrow \text{Fe(II)–As(V) complex} \quad (15)$$

$$\text{Fe(II)–As(III) complex} + H_2O_2 \rightarrow \text{Fe(III)–As(III) complex} \quad (16)$$

$$\text{Fe(II)–As(V) complex} + H_2O_2 \rightarrow \text{Fe(III)–As(V) complex} \quad (17)$$

$$\text{Fe(II)} + H_2O_2 \rightarrow \text{Fe(IV)} \quad (18)$$

$$\text{Fe(IV)} + \text{Fe(II)} \rightarrow 2\text{Fe(III)} \quad (19)$$

$$2\text{Fe(II)} + H_2O_2 \rightarrow 2\text{Fe(III)} \quad (20)$$

3.5. Oxidation of As(III) via reaction between Fe(III)–As(III) complexes and H_2O_2

To examine other pathways of As(III) oxidation not via Fe(IV), experiments were conducted to assess the effect of the Fe(III)–As(III) complex on As(III) oxidation in the presence of H_2O_2. Results in Fig. 5 show that As(III) was oxidized by H_2O_2 in the presence of Fe(III) at a nitrogen atmosphere. Of course, this part of As(III) oxidation cannot be attributed to HO• in the TBA scavenging experiment (Fig. S15). The log K value of the Fe(III)–(tiron)$_3$ complex is 46.9 (Naka et al., 2006), which is much higher than that of Fe(III)$(OH)_3$ (38.55). When excess tiron was added to the solution, As(III) cannot form the surface complex with Fe(III). Thus, tiron was added to the reaction solution to investigate the inhibitory effect. As expected, As(III) oxidation was completely inhibited by tiron (Fig. 5). This reaction may contribute little to the overall As(III) oxidation in the initial stage of As(III) and Fe(II) co-oxidation because both the reactants Fe(III)–As(III) complex and H_2O_2 are at very low concentrations. However, since excess DMSO can only inhibit about half of As(III) oxidation (Fig. 4b), the other half of As(III) oxidation most likely occurred via formation of the Fe(III)–As(III) complex and then directly underwent oxidization by H_2O_2 (eq (21)). The excess DMSO (400 mM) cannot inhibit As(III) oxidation in the presence of Fe(III) and H_2O_2 (Fig. S16), thus, the reaction in eq (21) occurred not via Fe(IV) on the CFH surface in neutral solution.

$$\text{Fe(III)–As(III) complex} + H_2O_2 \rightarrow \text{Fe(III)–As(V) complex} \quad (21)$$

3.6. Rate constants for reactions between Fe(III)/Fe(II)–As(III) complexes and H_2O_2

The pH metric titration method in the absence of oxygen as

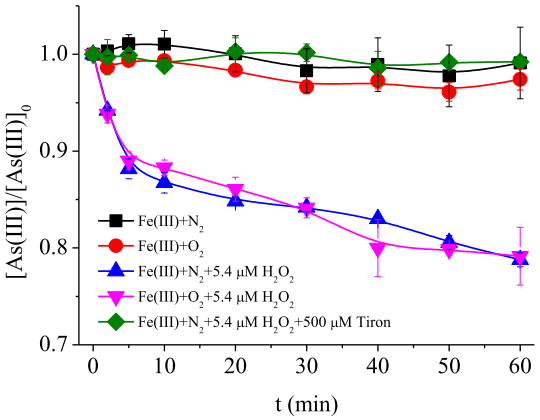

Fig. 5. Changes in As(III) concentrations in aqueous solutions containing Fe(III) with and without oxygen, H_2O_2 or both. Conditions: [As(III)] = 5 μM, [Fe(III)] = 50 μM, [PIPES] = 5 mM, [$NaNO_3$] = 10 mM, [H_2O_2] = 5.4 μM, [tiron] = 500 μM, pH 7.25.

proposed by Bjerrum (1941) and modified by Irving and Rossotti (1954) was applied in Fig. S17. The curves for Fe(II)–As(III) complex formation (Fig. 6a) extend to a maximum $\bar{n}$ value (ca. 2.7). The values of $\bar{n}$ ($0.20 < \bar{n}$) indicate that the complexes formed at least have 1:1 and 1:2 metal/ligand stoichiometry. However, the concentration of As(III) (5 μM) was much less than that used in Fig. 6a, thus only the 1:1 Fe(II)–As(III) complex was considered. The formation constant of Fe(II)–As(III) complex ($K_{Fe(II)-As(III)}$) calculated from the complex formation curves is $10^{3.86}$ M^{-1} (Fig. 6a) at half integrals using the Bjerrum's method (Bjerrum, 1941). Because the rates of As(III) oxidation through the reaction between the Fe(II)–As(III) complex and H_2O_2 ($r_{Fe(II)-As(III)}$) depends on the concentrations of Fe(II)–As(III) complex and H_2O_2, the rate of this reaction at various time is expressed as eq (22). Thus, $k_{Fe(II)-As(III)}$ was calculated to be 0.03 μM^{-1} min^{-1} shown in SI.

$$r_{Fe(II)-As(III)} = k_{Fe(II)-As(III)}[Fe(II)-As(III)] \times [H_2O_2] \quad (22)$$

In Fe(III) solution containing H_2O_2 and As(III) at neutral pH, As(III) oxidation occurs through the Fe(III)–As(III) complex as shown in eq (21) (the rate is expressed in eq (23)). A linear fit between the rates of As(III) oxidation via the Fe(III)–As(III) complex ($r_{Fe(III)-As(III)}$) and [Fe(III)–As(III)] × [H_2O_2] at various initial [H_2O_2] is evident in Fig. 6b. The rate constant of the reaction between Fe(III)–As(III) and H_2O_2, $k_{Fe(III)-As(III)}$, was determined to 0.03 μM^{-1} min^{-1}.

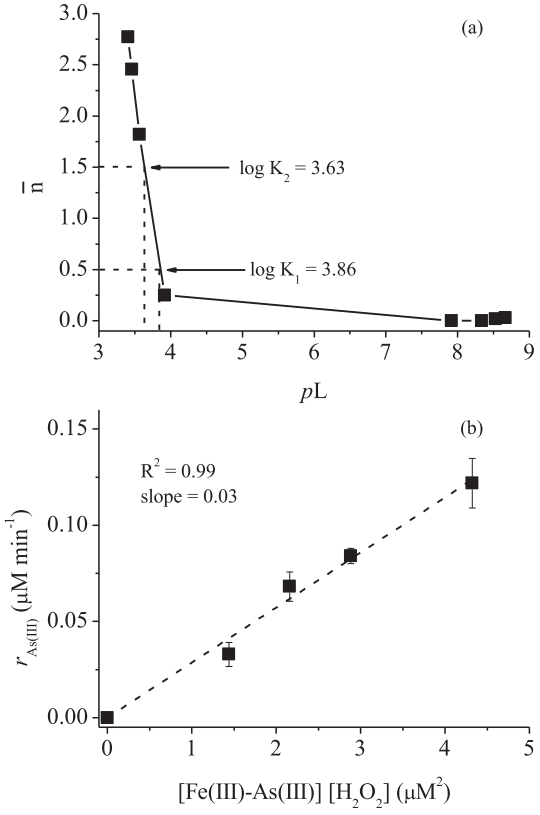

Fig. 6. (a) Formation curves of the Fe(II)–As(III) complex in a glove box filled with N_2. Conditions: [As(III)] = 4 mM, [Fe(II)] = 1 mM, [$NaNO_3$] = 100 mM, [HNO_3] = 10 mM, $[NaOH]_{addition}$ = 200 mM, T = 25 °C. $\bar{n}$, the average number of ligands attached per metal ion, and pL, the exponent for free ligand, were determined as described in the SI. (b) plot of the initial oxidation rates of As(III) ($r_{As(III)}$) versus [Fe(III)–As(III)] × [H_2O_2], where [Fe(III)–As(III)] was found to be 0.8 μM, with a formation constant of Fe(III)–As(III) complex at near-neutral pH. $K_{Fe(III)-As(III)} = 3.78 \times 10^3$ M^{-1} (Xu et al., 2014). Conditions: [As(III)] = 5 μM, [Fe(III)] = 50 μM, [PIPES] = 5 mM, [$NaNO_3$] = 10 mM, [H_2O_2] = 0–5.4 μM, pH 7.25.

$$r_{Fe(III)-As(III)} = k_{Fe(III)-As(III)}[Fe(III)-As(III)] \times [H_2O_2] \quad (23)$$

3.7. Mechanism integration

From the mass balance between dissolved and adsorbed As(III)/As(V) species, we determined the amounts of As(III) and As(V) adsorbed on CFH by centrifugation to separate the colloids in the samples without acidification. Fig. 7a shows that adsorption of either As(III) or the oxidized product As(V) is very fast. In particular, few As(V) could be detected in the supernatant solution at each sampling time because of the very strong adsorption of As(V) on the CFH ($K_{Fe(III)-As(V)} = 10^{22}$–$10^{27}$ M^{-1}) (Jia et al., 2006). The adsorption rate for As(III) was also high (ca. 0.015 μM min^{-1}); about 0.32 μM As(III) was adsorbed by CFH within 60 min. Fig. 7a also suggests that dissolved Fe(II) became depleted quickly not only because of oxidation but also because of adsorption onto CFH, which enables Fe(II)–As(III) oxidation on the surface of CFH possible.

The overall rates of As(III) oxidation ($r_{As(III)}$), $r_{Fe(II)-As(III)}$ calculated by eq (22) and $r_{Fe(III)-As(III)}$ calculated by eq (23) at each sampling point can be compared in Fig. 7b. The result suggests that $r_{Fe(II)-As(III)}$ is crucial at the initial stage of the reaction and that $r_{Fe(III)-As(III)}$ accounts for only less than 10% of $r_{As(III)}$ at 5 min. However, the As(III) oxidation through Fe(III)–As(III) complex becomes the major pathway in the middle and final stages of As(III) oxidation. The sum of $r_{Fe(II)-As(III)}$ and $r_{Fe(III)-As(III)}$ is approximately equal to $r_{As(III)}$, which confirms the dependence of As(III) oxidation by H_2O_2 on Fe(II)–As(III) and Fe(III)–As(III) complexations in Fe(II) solutions. Accordingly, the proposed process of As(III) and Fe(II) co-oxidation by oxygen at neutral pH is shown in Scheme 1.

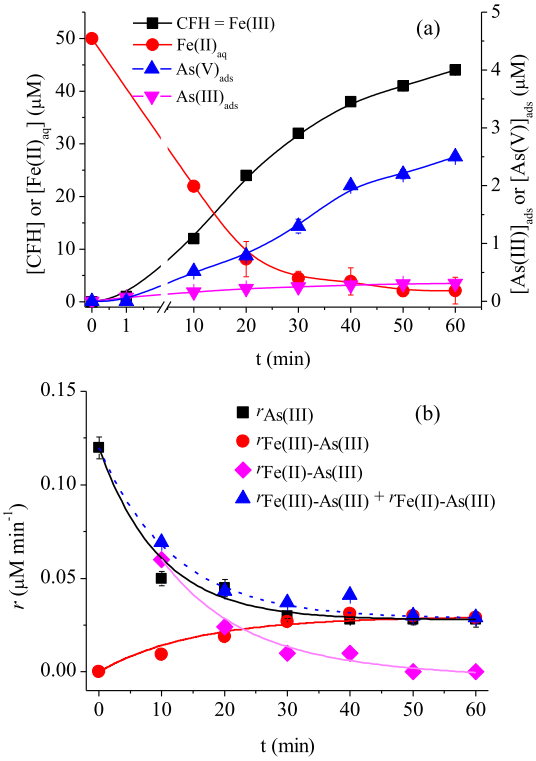

Fig. 7. (a) Changes in concentrations of Fe(III) (CFH), dissolved Fe(II) ($Fe(II)_{aq}$), adsorbed As(III) ($As(III)_{ads}$), and As(V) ($As(V)_{ads}$) on CFH during co-oxidation of As(III) and Fe(II). (b) Changes in rates of As(III) oxidation via the Fe(II)–As(III) complex (path 1) and Fe(III)–As(III) (path 2) during co-oxidation of As(III) and Fe(II). Conditions: [As(III)] = 5 μM, [Fe(II)] = 50 μM, [PIPES] = 5 mM, [$NaNO_3$] = 10 mM, pH 7.25.

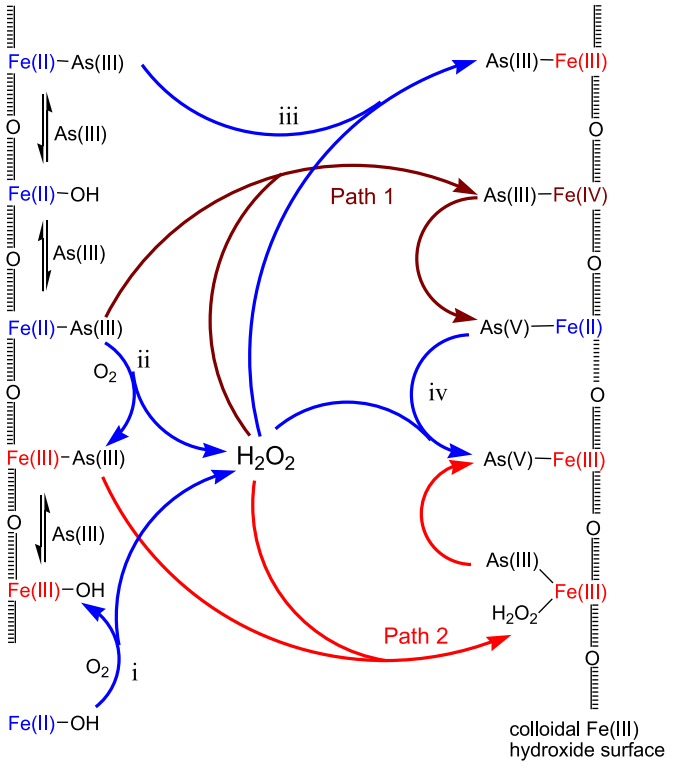

Scheme 1. Proposed co-oxidation processes of As(III) and Fe(II) through the formation of Fe(II)/Fe(III)–As(III)/As(V) complexes at neutral pH in the presence of O_2. As(III) oxidation pathways are marked by numbers 1 and 2. Fe(II) oxidation pathways are maked by numbers i–iv. For simplification, the possible Fe(II)–As(III) complex reaction in bulk solution (in pathway 1) is not presented; O atoms in various Fe(II)/Fe(III)–As(III)/As(V) complexes are omitted.

4. Conclusion

This work investigated the co-oxidation of As(III) and Fe(II) in the presence of O_2 at neutral solutions, and revealed the importance of complexation between Fe(II)/Fe(III) and As(III)/As(V) sepcies for the co-oxidation of As(III) and Fe(II). The oxidation of the Fe(II)–As(III) complex promotes the production of H_2O_2, which oxidizes As(III) through the Fe(II)/Fe(III)–As(III) complexes. The H_2O_2 reacts with the Fe(II)–As(III) complex via the intermediate Fe(IV), which contributes to approximately half of As(III) oxidation. The other half of As(III) oxidation by H_2O_2 occurs via intramolecular electrons transfer after the formation of Fe(III)–As(III) complexes. The complexation between Fe(II)/Fe(III) and As(III)/As(V) sepcies at neutral pH presents an overlooked mechanism of co-oxidation of As(III) and Fe(II), which supplements the fundamentals for the oxidation behaviors of As(III) in natural water (e.g. groundwater) and offers the new viewpoint on neutral Fenton and Fenton-like systems used as advanced oxidation processes for the treatment of arsenite-containing water.

Acknowledgments

This work was financially supported by National Natural Science Foundation of China (No. 21477090 and 21777125), Science and Technology Project of Guangdong Province (No. 2014B030301055 and 2016B020242006).

Appendix A. Supplementary data

Supplementary data related to this article can be found at https://doi.org/10.1016/j.watres.2018.06.072.

References

Banerjee, K., Amy, G.L., Prevost, M., Nour, S., Jekel, M., Gallagher, P.M., Blumenschein, C.D., 2008. Kinetic and thermodynamic aspects of adsorption of arsenic onto granular ferric hydroxide (GFH). Water Res. 42 (13), 3371–3378.
Bataineh, H., Pestovsky, O., Bakac, A., 2012. pH-induced mechanistic changeover from hydroxyl radicals to iron(IV) in the Fenton reaction. Chem. Sci. 3 (5), 1594–1599.
Biaglow, J.E., Kachur, A.V., 1997. The generation of hydroxyl radicals in the reaction of molecular oxygen with polyphosphate complexes of ferrous ion. Radiat. Res. 148 (2), 181–187.
Bjerrum, J., 1941. Metal Ammine Formation in Aqueous Solution. P. Hasse and Sons, Copenhagen.
Goldberg, S., 2002. Competitive adsorption of arsenate and arsenite on oxides and clay minerals. Soil Sci. Soc. Am. J. 66 (2), 413–421.
Hug, S.J., Canonica, L., Wegelin, M., Gechter, D., Von Gunten, U., 2001. Solar oxidation and removal of arsenic at circumneutral pH in iron containing waters. Environ. Sci. Technol. 35 (10), 2114–2121.
Hug, S.J., Leupin, O., 2003. Iron-catalyzed oxidation of arsenic(III) by oxygen and by hydrogen peroxide: pH-dependent formation of oxidants in the Fenton reaction. Environ. Sci. Technol. 37 (12), 2734–2742.
Irving, H.M., Rossotti, H.S., 1954. The calculation of formation curves of metal complexes from pH titration curves in mixed solvents. J. Chem. Soc. 3397 (4), 2904–2910.
Jia, Y.F., Xu, L.Y., Fang, Z., Demopoulos, G.P., 2006. Observation of surface precipitation of arsenate on ferrihydrite. Environ. Sci. Technol. 40 (10), 3248–3253.
Johnston, R.B., Singer, P.C., 2007. Redox reactions in the Fe-As-O_2 system. Chemosphere 69 (4), 517–525.
Jones, A.M., Griffin, P.J., Waite, T.D., 2015. Ferrous iron oxidation by molecular oxygen under acidic conditions: the effect of citrate, EDTA and fulvic acid. Geochem. Cosmochim. Acta 160, 117–131.
Katsoyiannis, I.A., Ruettimann, T., Hug, S.J., 2008. pH dependence of Fenton reagent generation and As(III) oxidation and removal by corrosion of zero valent iron in aerated water. Environ. Sci. Technol. 42 (19), 7424–7430.
Katsoyiannis, I.A., Voegelin, A., Zouboulis, A.I., Hug, S.J., 2015. Enhanced As(III) oxidation and removal by combined use of zero valent iron and hydrogen peroxide in aerated waters at neutral pH values. J. Hazard Mater. 297, 1–7.
Keenan, C.R., Sedlak, D.L., 2008. Factors affecting the yield of oxidants from the reaction of manoparticulate zero-valent iron and oxygen. Environ. Sci. Technol. 42 (4), 1262–1267.
Lee, J., Kim, J., Choi, W., 2014. Oxidation of aquatic pollutants by ferrous-oxalate complexes under dark aerobic conditions. J. Hazard Mater. 274, 79–86.
Li, J., Ma, W.H., Huang, Y.P., Tao, X., Zhao, J.C., Xu, Y.M., 2004. Oxidative degradation of organic pollutants utilizing molecular oxygen and visible light over a supported catalyst of $Fe(bpy)_3^{2+}$ in water. Appl. Catal. B Environ. 48, 17–24.
Manning, B.A., Fendorf, S.E., Goldberg, S., 1998. Surface structures and stability of arsenic(III) on goethite: spectroscopic evidence for inner-sphere complexes. Environ. Sci. Technol. 32 (16), 2383–2388.
Millo, F.J., 1985. The effect of ionic interactions on the oxidation of metals in natural waters. Geochem. Cosmochim. Acta 49 (2), 547–553.
Naka, D., Kim, D., Strathmann, T.J., 2006. Abiotic reduction of nitroaromatic compounds by aqueous iron(II)–catechol complexes. Environ. Sci. Technol. 40 (9), 3006–3012.
Ona-Nguema, G., Morin, G., Wang, Y., Foster, A.L., Juillot, F., Calas Jr., G., Brown, G.E., 2010. XANES evidence for rapid arsenic(III) oxidation at magnetite and ferrihydrite surfaces by dissolved O_2 via Fe^{2+}-mediated reactions. Environ. Sci. Technol. 44 (14), 5416–5422.
Ona-Nguema, G., Morin, G., Wang, Y., Menguy, N., Juillot, F., Olivi, L., Aquilanti, G., Abdelmoula, M., Ruby, C., Bargar, J.R., Guyot, F., Calas Jr., G., Brown, G.E., 2009. Arsenite sequestration at the surface of nano-$Fe(OH)_2$, ferrous-carbonate hydroxide, and green-rust after bioreduction of arsenic-sorbed lepidocrocite by *Shewanella putrefaciens*. Geochem. Cosmochim. Acta 73 (5), 1359–1381.
Oremland, R.S., Stolz, J.F., 2003. The ecology of arsenic. Science 300 (5621), 939–944.
Pang, S., Jiang, J., Ma, J., 2011. Oxidation of sulfoxides and arsenic(III) in corrosion of nanoscale zero valent iron by oxygen: evidence against ferryl ions (Fe(IV)) as active intermediates in Fenton reaction. Environ. Sci. Technol. 45 (7), 307–312.
Raven, P.K., Jain, A., Loeppert, R.H., 1998. Arsenite and arsenate adsorption on ferrihydrite: kinetics, equilibrium, and adsorption envelopes. Environ. Sci. Technol. 3 (32), 344–349.
Shao, B.B., Guan, Y.Y., Tian, Z.Y., Guan, X.H., Wu, D.L., 2016. Advantages of aeration in arsenic removal and arsenite oxidation by structural Fe(II) hydroxides in aqueous solution. Colloid. Surface. Physicochem. Eng. Aspect. 506, 703–710.
Sorg, T.J., Chen, A.S.C., Wang, L., 2014. Arsenic species in drinking water wells in the USA with high arsenic concentrations. Water Res. 48 (1), 156–169.
Speight, J.G., 2005. Lange's Chemistry Handbook. McGraw-Hill, New York, p. 345.
Stumm, W., Lee, G.F., 1961. Oxygenation of ferrous iron. Ind. Eng. Chem. 53 (2), 143–146.
Thoral, S., Rose, J., Garnier, J.M., Van Geen, A., Refait, P., Traverse, A., Fonda, E., Nahon, D., Bottero, J.Y., 2005. XAS study of iron and arsenic speciation during Fe(II) oxidation in the presence of As(III). Environ. Sci. Technol. 39 (24), 9478–9485.

Wang, Y.J., Xu, J., Li, J.J., Wu, F., 2013. Natural montmorillonite induced photooxidation of As(III) in aqueous suspensions: roles and sources of hydroxyl and hydroperoxyl/superoxide radicals. J. Hazard Mater. 260 (18), 255–262.
Weiss, J., 1935. Elektronenübergangsprozesse im mechanismus von oxydations- und reduktionsreaktionen in lösungen. Naturwissenschaften 23 (4), 64–69.
Weiss, J., 1953. The autoxidation of ferrous ions in aqueous solution. Experientia 9 (2), 61–62.
Welch, K.D., Davis, T.Z., Aust, S.D., 2002. Iron autoxidation and free radical generation: effects of buffers, ligands, and chelators. Arch. Biochem. Biophys. 397 (2), 360–369.
Wood, P.M., 1988. The potential diagram for oxygen at pH 7. Biochem. J. 253 (1), 287–289.
Xu, J., Li, J.J., Wu, F., Zhang, Y., 2014. Rapid photooxidation of As(III) through surface complexation with nascent colloidal ferric hydroxide. Environ. Sci. Technol. 48 (1), 272–278.